

## Mechanisms and Applications of Plasmon-Induced Charge Separation at TiO<sub>2</sub> Films Loaded with Gold Nanoparticles

Yang Tian and Tetsu Tatsuma\*

Contribution from the Institute of Industrial Science, The University of Tokyo, 4-6-1 Komaba, Meguro-ku, Tokyo 153-8505, Japan

Received December 28, 2004; E-mail: tatsuma@iis.u-tokyo.ac.jp

**Abstract:** Plasmon-induced photoelectrochemistry in the visible region was studied at gold nanoparticle–nanoporous TiO<sub>2</sub> composites (Au–TiO<sub>2</sub>) prepared by photocatalytic deposition of gold in a porous TiO<sub>2</sub> film. Photoaction spectra for both the open-circuit potential and short-circuit current were in good agreement with the absorption spectrum of the gold nanoparticles in the TiO<sub>2</sub> film. The gold nanoparticles are photoexcited due to plasmon resonance, and charge separation is accomplished by the transfer of photoexcited electrons from the gold particle to the TiO<sub>2</sub> conduction band and the simultaneous transfer of compensative electrons from a donor in the solution to the gold particle. Besides its low-cost and facile preparation, a photovoltaic cell with the optimized electron mediator (Fe<sup>2+/3+</sup>) exhibits an optimum incident photon to current conversion efficiency (IPCE) of 26%. The Au–TiO<sub>2</sub> can photocatalytically oxidize ethanol and methanol at the expense of oxygen reduction under visible light; it is potentially applicable to a new class of photocatalysts and photovoltaic fuel cells.

### Introduction

Metal nanoparticles are of great interest because of their unique electronic, optical, and magnetic properties.<sup>1–5</sup> In particular, nanoparticles of noble metals such as gold and silver have been attracting more attention<sup>6–8</sup> because they have many color varieties in the visible region based on plasmon resonance, which is due to the collective oscillations of the electrons at the surface of the nanoparticles. The resonance wavelength strongly depends on the size and shape of the nanoparticles, the interparticle distance, and the dielectric property of the surrounding medium. The unique plasmon absorbance features of these noble metal nanoparticles have been exploited for a wide variety of applications<sup>9</sup> including chemical sensors and biosensors. Plasmon-induced photochemical reactions have also been employed to produce silver nanoprisms and gold nanorods.<sup>7,8,10,11</sup> Photoinduced “melting” of gold nanorods, which is likely based on nonradiative deactivation of the plasmon, has

been exploited for irreversible writing of an image.<sup>12</sup> We have reported reversible photoinduced multicolor imaging (multicolor photochromism) of silver nanoparticles deposited in a nanoporous TiO<sub>2</sub> film by photocatalytic means.<sup>13,14</sup>

However, charge separation at a plasmon-excited metal nanoparticle without degradation (e.g., corrosion) of the particle has never been reported to the best of our knowledge. If this is possible, photovoltaic cells<sup>15</sup> with expensive organic dyes and inorganic dyes with organic ligands would be improved in terms of cost and stability. A new class of visible light-sensitive photocatalysts and photovoltaic fuel cells are additional potential applications. Although metal nanoparticles have been employed in photocatalysts<sup>16</sup> and photovoltaic cells,<sup>17</sup> the particles have not been used as photosensitizers.

Although Kozuka et al.<sup>18</sup> have observed anodic photocurrents in response to visible light irradiation at gold- and silver-deposited TiO<sub>2</sub> films, the stability of the metals is unknown. In addition, they had to apply a large bias voltage to obtain action spectra because they did not add an appropriate electron donor. Recently, we have reported photoelectrochemistry at gold and silver nanoparticles incorporated in nanoporous TiO<sub>2</sub>.<sup>19</sup> We have developed almost, but not completely, stable systems by combining it with an electron donor (I<sup>–</sup>) and demonstrated

- (1) Murry, C. B.; Kagan, C. R.; Bawendi, M. G. *Science* **1995**, *270*, 1335–1338.
- (2) Ziole, R. F.; Giannelis, E. P.; Weinstein, B. A.; O'Horo, M. P.; Ganguly, B. N.; Mehrotra, V.; Russell, M. W.; Huffmann, D. R. *Science* **1992**, *257*, 219–223.
- (3) Kang, Y. S.; Risbud, S.; Rabolt, J. F.; Stroeve, P. *Chem. Mater.* **1996**, *8*, 2209–2211.
- (4) Collier, C. P.; Saykally, R. J.; Shiang, J. J.; Henrichs, S. E. H. J. R. *Science* **1997**, *277*, 1978–1981.
- (5) Zhao, M.; Sun, L.; Crooks, R. M. *J. Am. Chem. Soc.* **1998**, *120*, 4877–4878.
- (6) Link, S.; El-Sayed, M. A. *J. Phys. Chem. B* **1999**, *103*, 8410–8426.
- (7) Jin, R.; Cao, Y. C.; Mirkin, C. A.; Kelly, K. L.; Schatz, G. C.; Zheng, J. G. *Science* **2001**, *294*, 1901–1903.
- (8) Mock, J. J.; Barbic, M.; Smith, D. R.; Schultz, D. A.; Schultz, S. *J. Chem. Phys.* **2002**, *116*, 6755–6759.
- (9) Daniel, M.-C.; Astruc, D. *Chem. Rev.* **2004**, *104*, 293–346.
- (10) Jin, R.; Cao, Y. C.; Hao, E.; Métraux, G. S.; Schatz, G. C.; Mirkin, C. A. *Nature* **2003**, *425*, 487–490.
- (11) Kim, F.; Song, J. H.; Yang, P. *J. Am. Chem. Soc.* **2002**, *124*, 14316–14317.

- (12) Wilson, B. O.; Wilson, G. J.; Mulvaney, P. *Adv. Mater.* **2002**, *14*, 1000–1004.
- (13) Ohko, Y.; Tatsuma, T.; Fujii, T.; Naoi, K.; Niwa, C.; Kubota, Y.; Fujishima, A. *Nature Mater.* **2003**, *2*, 29–31.
- (14) Naoi, K.; Ohko, Y.; Tatsuma, T. *J. Am. Chem. Soc.* **2004**, *126*, 3664–3668.
- (15) Grätzel, M. *Nature* **2001**, *414*, 338–344.
- (16) Bard, A. J. *J. Phys. Chem.* **1982**, *86*, 172–177.
- (17) Subramanian, V.; Wolf, E.; Kamat, P. V. *J. Phys. Chem. B* **2001**, *105*, 11439–11446.
- (18) Zhao, G.; Kozuka, H.; Yoko, T. *Thin Solid Films* **1996**, *277*, 147–154.
- (19) Tian, Y.; Tatsuma, T. *Chem. Commun.* **2004**, 1810–1811.

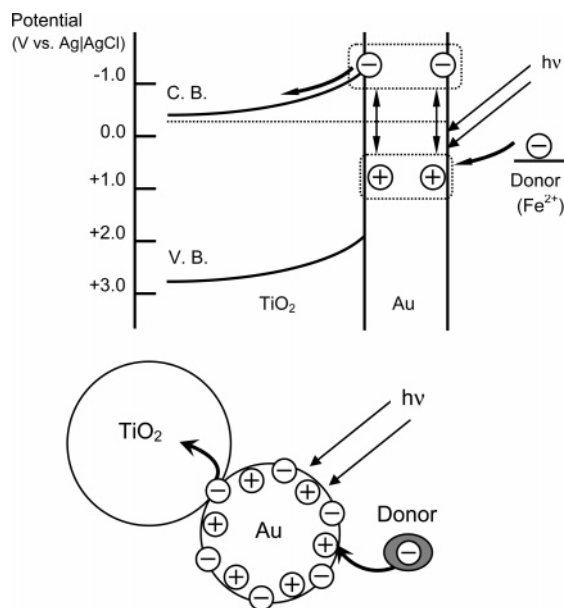


**Figure 1.** Proposed mechanism for the photoelectrochemistry. Charges are separated at a visible-light-irradiated gold nanoparticle–TiO<sub>2</sub> system.

complete matching between the plasmon absorption spectra of the metal nanoparticles and photopotential and photocurrent action spectra obtained without bias voltage. Thus we have verified that our system is potentially applicable to inexpensive photovoltaic cells and visible-light-sensitive photocatalysts.

However, the mechanism is still unknown, and as a photovoltaic cell, the incident photon to current conversion efficiency (IPCE) was too low (1% for Au–TiO<sub>2</sub>) for practical applications. In the present work, we examined a series of donors for the Au–TiO<sub>2</sub> and the IPCE was improved by a factor of >20. Also, we found that the Au–TiO<sub>2</sub> is potentially applicable to visible-light-induced photocatalytic oxidation of ethanol and methanol and reduction of oxygen. In addition, we studied the mechanism of the system and evidenced that the photoelectrochemistry is based on the charge separation at the gold nanoparticles, which includes electron transfer from the plasmon-excited gold to TiO<sub>2</sub> and that from a donor to the gold (Figure 1).

## Experimental Section

**Chemicals and Materials.** Acetonitrile (analytical grade), ethylene glycol (analytical grade), lithium nitrate, iron(II) chloride, potassium iodide, potassium chloride, ethanol (99.5%), and methanol (99.5%) were purchased from Wako Pure Chemical Industries, Ltd. (Osaka, Japan) and used as supplied. Iron(III) chloride, potassium bromide, and potassium ferrocyanide were purchased from Kanto Chemical Co., Inc. (Tokyo, Japan). Ferrocenecarboxylic acid and 1,1'-ferrocenedicarboxylic acid were obtained from Aldrich Chemical Co., Inc. and used without further purification. The solution used in this work was freshly prepared and deoxygenated by bubbling nitrogen gas for at least 30 min prior to use.

**Preparations of TiO<sub>2</sub> and Au–TiO<sub>2</sub> Films.** A TiO<sub>2</sub> film was prepared as follows: an ITO-coated glass plate was coated with a nanoporous TiO<sub>2</sub> film prepared from an anatase TiO<sub>2</sub> sol (Ishihara Sangyo Kaisha, STS-21, 20 nm particle diameter) by spin-coating (sintered at 723 K for 1 h). The film thickness was 4 μm. A thicker TiO<sub>2</sub> film (10 μm) employed in the measurements of total energy conversion efficiency was prepared from TiO<sub>2</sub> paste (Pecell Technologies, Japan) by the squeegee method and sintered at 423 K for 15 min. The former TiO<sub>2</sub> film was used unless otherwise noted. For the

preparation of a Au–TiO<sub>2</sub> film, we employed a photocatalytic reduction method widely reported for the preparation of metal nanoparticles (e.g., Pt, Cu, Ag, Pd, and Au) on TiO<sub>2</sub> films.<sup>13,14,20,21</sup> A TiO<sub>2</sub> film was soaked in 5 mM aqueous HAuCl<sub>4</sub> for about 30 min and rinsed with water. Then, the film was irradiated with ultraviolet light (1 mW cm<sup>-2</sup>) for at least 1 h to reduce the adsorbed Au<sup>3+</sup> to Au by TiO<sub>2</sub> photocatalysis at the expense of water oxidation.

**Instruments and Measurements.** The UV absorption spectra of the films were measured using a UV spectrophotometer (UV-2400PC, Shimadzu, Japan). An HZ 3000 automatic polarization system (Hokuto Denko, Japan) was employed in electrochemical measurements. Photoaction spectra for the potential changes were obtained in a conventional two-compartment three-electrode electrochemical cell. The reference electrode was a KCl-saturated Ag|AgCl electrode, while the auxiliary electrode was a platinum wire. To test the performance of each electron donor, a platinum wire was employed as the counter electrode in a two-compartment two-electrode cell. On the other hand, action spectra for the photocurrent changes and energy conversion efficiency were obtained in a two-electrode sandwich cell (thickness of the electrolyte, 5 mm). The counter electrode was a gold film sputtered on an ITO-coated glass plate. The Au–TiO<sub>2</sub> substrate was irradiated with a white light ( $\lambda > 420$  or 500 nm) using a xenon lamp with an ultraviolet-cutoff filter from the back. Action spectra were collected using a xenon lamp with an appropriate band-pass filter (fwhm, 10 nm) or a M25 monochromator (fwhm, 20 nm) (Bunkou Keiki, Japan). A Hitachi S-4500 (Japan) scanning electron microscope (SEM) was employed to record the images with 100 K magnifications. The structures of TiO<sub>2</sub> and Au–TiO<sub>2</sub> films were analyzed by X-ray photoelectron spectroscopy (XPS) using a Quantum-2000 Scanning ESCA microprobe (ULVAC-PHI, Inc.) with Mg K $\alpha$  radiation.

## Results and Discussion

**Characterization of the Au–TiO<sub>2</sub> Film.** The visible absorption spectrum of gold deposited in the nanoporous TiO<sub>2</sub> film was clearly characterized by the plasmon resonance peak of gold nanoparticles (Figure 2B, curve b). In comparison with commercially available gold nanoparticles (AuE-101, 5–20 nm diameter, Nippon Paint) suspended in ethanol (Figure 2B, curve a), the peak of the photocatalytically deposited one was red-shifted and broadened due to the high refractive index of anatase TiO<sub>2</sub> (2.52).<sup>22</sup> Another possible explanation might be formation of an indirect charge transfer band.<sup>23</sup> Incidentally, apparent absorption of the unmodified TiO<sub>2</sub> film in the visible region (Figure 2A) should be ascribed to light scattering, because the film was not visibly colored before the deposition of gold.

We verified that the deposited gold was metallic by X-ray photoelectron spectroscopy (XPS) (inset of Figure 2A). The peaks observed at 84.0 and 87.7 eV were ascribed to metallic gold. In addition, the diameter of the particles observed in SEM images of the present Au–TiO<sub>2</sub> film was less than 50 nm (inset of Figure 2B). Thus, we can conclude that nanosized gold particles are formed in the TiO<sub>2</sub> film. Also, XPS measurements combined with film etching proved that the gold nanoparticles were distributed in the whole film, although the particles were somewhat concentrated in the surface region.

**Dependence of the Photovoltaic Performance on the Donor.** As we have reported previously, the Au–TiO<sub>2</sub> can be

(20) Kraeutler, B.; Bard, A. J. *J. Am. Chem. Soc.* **1978**, *100*, 4317–4318.

(21) Subramanian, V.; Wolf, E. E.; Kamat, P. V. *Langmuir* **2003**, *19*, 469–474.

(22) Fujishima, A.; Hashimoto, K.; Watanabe, T. *TiO<sub>2</sub> photocatalysis: fundamentals and applications*; BKC: Tokyo, 1999; p 125.

(23) Yang, M.; Thompson, D. W.; Meyer, G. J. *Inorg. Chem.* **2002**, *41*, 1254–1262.

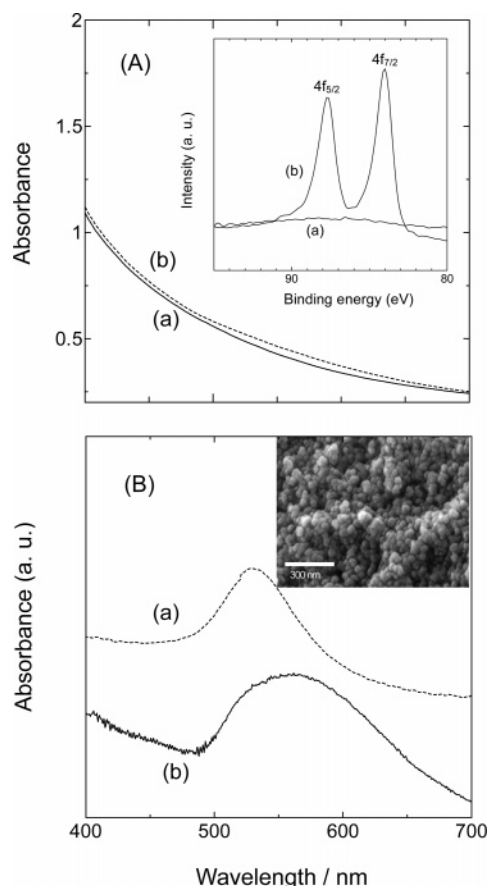


**Figure 2.** Absorption spectra of (A-a) the nanoporous  $\text{TiO}_2$  film, (A-b)  $\text{Au-TiO}_2$  film (gold nanoparticles were deposited by photocatalytical means), (B-a) commercially available gold nanoparticles suspended in ethanol, and (B-b) gold nanoparticles deposited photocatalytically in the  $\text{TiO}_2$  film (the spectrum of  $\text{TiO}_2$  has been subtracted). Inset in A: X-ray photoelectron spectra of the  $\text{TiO}_2$  (a) and  $\text{Au-TiO}_2$  (b) films. Inset in B: SEM image of the  $\text{Au-TiO}_2$  film (cross sectional view).

used as a photoanode when it is combined with  $\text{I}^-$  as an electron donor. However, the open-circuit photovoltage was 0.125 V and IPCE was about 1%. To improve these characteristics, we have to optimize the donor and its concentration. The use of the  $\text{I}^-/\text{I}_3^-$  couple is also disadvantageous from the viewpoint of stability because of its corrosive property toward metals including gold.  $[\text{Fe}(\text{CN})_6]^{4-}$ ,  $\text{I}^-$ ,  $\text{Fe}^{2+}$ , ferrocenecarboxylic acid,  $\text{Br}^-$ , 1,1'-ferrocenedicarboxylic acid, and  $\text{Cl}^-$  were examined as electron donors. The apparent formal potential  $E'^{\text{app}}$  of each donor was evaluated by cyclic voltammetry as the average of anodic and cathodic peak potentials obtained at a platinum electrode [ $E'^{\text{app}} = (E_{\text{p,a}} + E_{\text{p,c}})/2$ ].

Photoelectrochemical measurements were performed with a cell with a  $\text{Au-TiO}_2$  photoanode, a platinum wire cathode, and a  $\text{N}_2$ -saturated acetonitrile and ethylene glycol (v/v 60/40) solution containing 0.1 M lithium nitrate and 0.1 M donor. The dependencies of open-circuit photovoltage ( $V_{\text{oc}}$ ) and short-circuit photocurrent density ( $J_{\text{sc}}$ ) on the apparent formal potential of different donors are plotted in Figure 3. The open-circuit photovoltage increased linearly as the apparent formal potential shifted positively and then became almost constant. The increase is explained in terms of a simple positive shift in the platinum counter electrode potential with the apparent formal potential. The saturation might be due to suppression of photopotential with decelerated electron transfer from the donor to the hole in

the gold particle and accelerated back electron transfer from the gold or  $\text{TiO}_2$  conduction band to the oxidized donor. In any event, the maximum photovoltage of the present cell is about 0.75 V.

The kinetics is more clearly reflected by the dependence of the short-circuit photocurrents on the redox potential of the donor/acceptor (acceptor = oxidized donor) couple (Figure 3B). It is obvious that there is an optimum potential for the donor/acceptor redox couple (i.e., electron mediator). The potential should be more negative than that of the hole on the gold nanoparticle; otherwise the donor (reduced mediator) cannot give electrons to the nanoparticles. On the other hand, the potential should be more positive than that of the  $\text{TiO}_2$  conduction band; otherwise the acceptor (oxidized mediator) cannot receive electrons from the gold nanoparticles via  $\text{TiO}_2$  and the counter electrode. Among the donors examined,  $\text{Fe}^{2+}$  is the best one since it leads to the largest photocurrent ( $46 \mu\text{A cm}^{-2}$ ) and an almost optimum photovoltage (0.68 V). It is possible that some ligands coordinate to  $\text{Fe}^{2+/3+}$  and the complex provides the optimal performances.

To fabricate the cell with better performance, the concentration ratio of  $\text{Fe}^{2+}$  to  $\text{Fe}^{3+}$  and the proportion between acetonitrile and ethylene glycol in solvent were optimized. When  $\text{FeCl}_2$  and  $\text{FeCl}_3$  concentrations were 0.1 and 0.05 M, respectively, the highest photocurrent and total energy conversion efficiency were obtained. The Nernstian potential was measured at a gold electrode in the electrolyte used and found to be  $0.46 \pm 0.02$  V, which is almost the same as the theoretical value of 0.46 V. The optimal composition of the solvent was 60 vol % acetonitrile and 40 vol % ethylene glycol. In addition, the photocurrent changes obtained after consecutive measurements in this solution for more than 3 days did not exceed 8%. The photoelectrochemical performance exhibited here was stable and reproducible.

**Optimized Photovoltaic Cell Performance.** Action spectra of the optimized photovoltaic cell were compared with the absorption spectrum of the gold nanoparticles incorporated into the  $\text{TiO}_2$  film (Figure 4, solid curves). The photopotential action spectra of the  $\text{Au-TiO}_2$  film obtained in  $\text{N}_2$ -saturated acetonitrile and ethylene glycol (v/v 60/40) solution containing 0.1 M lithium nitrate are depicted in Figure 4A. A remarkable negative shift of the open-circuit potential was observed at the  $\text{Au-TiO}_2$  film under monochromatic visible light illumination, while no obvious change was obtained at a  $\text{TiO}_2$  film as reported in our previous work<sup>19</sup> because  $\text{TiO}_2$  absorbs only UV light. The maximum potential response ( $\sim 170$  mV) was observed exactly at the absorption peak wavelength. The action spectrum for potential changes was in good agreement with the absorption spectrum of gold nanoparticles incorporated into the  $\text{TiO}_2$  film; the negative potential shift under visible light irradiation was ascribed to the surface plasmon absorption of the gold nanoparticles.

The short-circuit currents were also obtained at the  $\text{Au-TiO}_2$  film under visible light illumination in the presence of the redox couple  $\text{FeCl}_2/\text{FeCl}_3$ . An increased anodic photocurrent was observed as the visible light was turned on and the current almost returned to the background when irradiation was ceased. IPCE was evaluated from the short-circuit photocurrent as shown in Figure 4B. The photocurrent action spectrum coincided very well with the absorption spectrum of gold nanoparticles in the

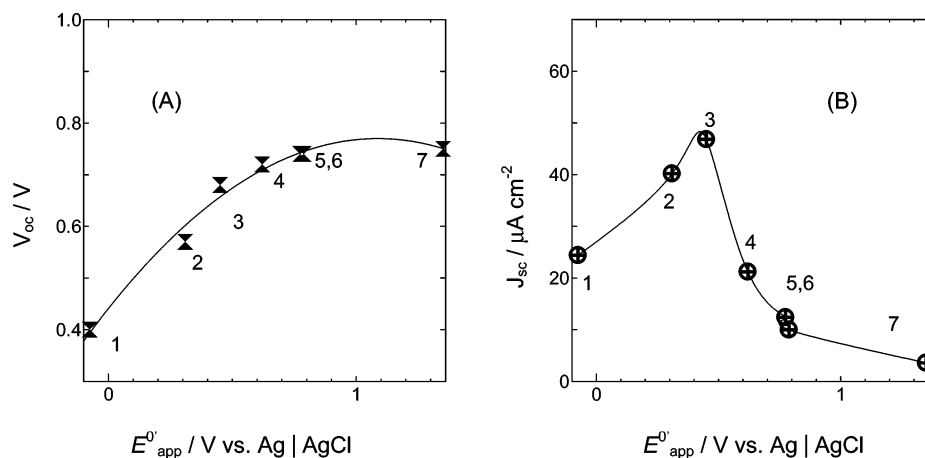


**Figure 3.** Plots of (A) open-circuit photovoltages and (B) short-circuit photocurrent densities vs apparent formal potential of different donors (1, [Fe(CN)<sub>6</sub>]<sup>4-</sup>; 2, I<sup>-</sup>; 3, Fe<sup>2+</sup>; 4, ferrocenecarboxylic acid; 5, Br<sup>-</sup>; 6, 1,1'-ferrocenedicarboxylic acid; 7, Cl<sup>-</sup>) for the cell with the Au–TiO<sub>2</sub> photoanode, a Pt cathode, and acetonitrile and ethylene glycol (v/v 60/40) containing 0.1 M LiNO<sub>3</sub> and 0.1 M donor. The anode was irradiated with a Xe lamp with a UV-cutoff filter (10 mW cm<sup>-2</sup>).

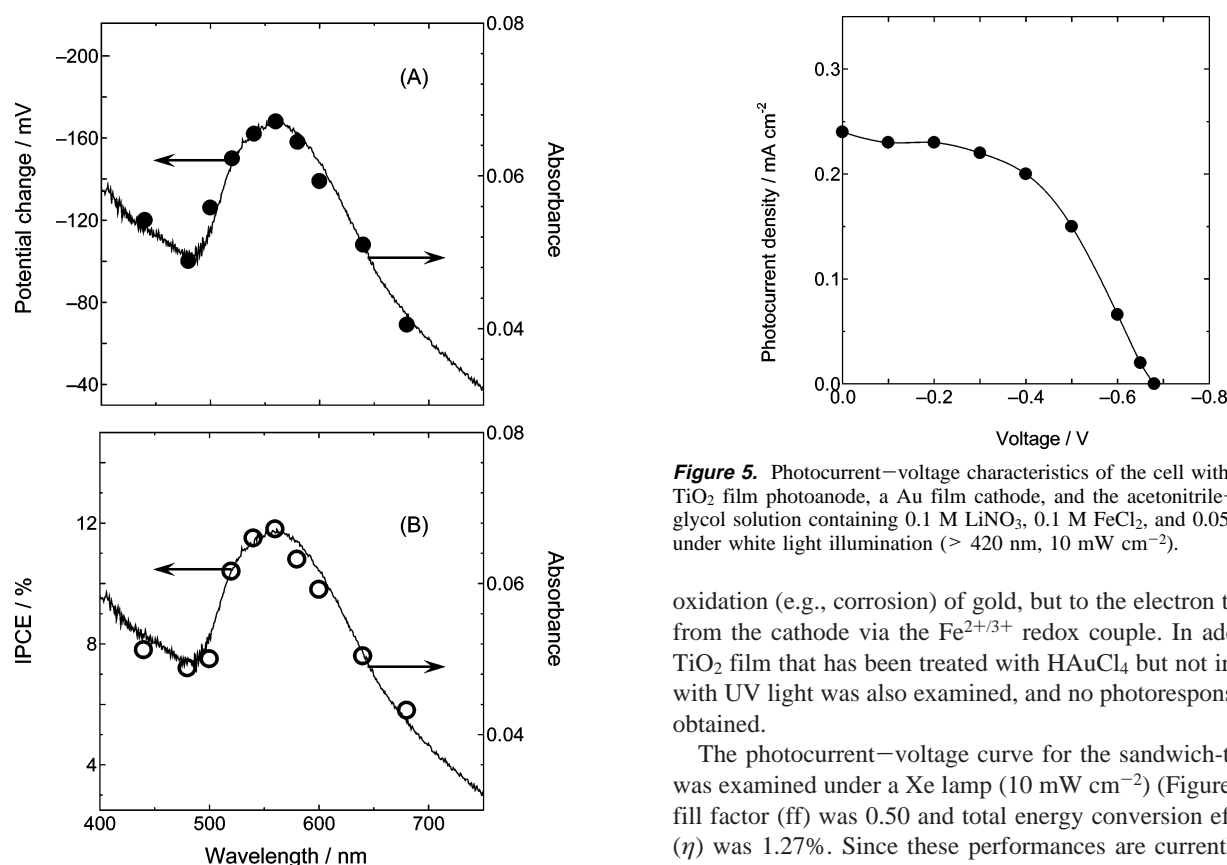


**Figure 4.** Action spectra for changes in open-circuit potential (A) and IPCE (B) of the Au–TiO<sub>2</sub> film in a N<sub>2</sub>-saturated acetonitrile and ethylene glycol (v/v: 60/40) solution containing 0.1 M LiNO<sub>3</sub> and (B) 0.1 M FeCl<sub>2</sub> and 0.05 M FeCl<sub>3</sub> in response to visible light irradiation ( $1.36 \times 10^{14}$  photons cm<sup>-2</sup> at each wavelength). A conventional cell was employed in the measurements of open-circuit potential with a KCl-saturated Ag|AgCl reference electrode. A two-electrode sandwich cell (thickness of electrolyte, 5 mm) was used in the measurements of IPCE with a Au film cathode.

TiO<sub>2</sub> film and showed the maximum IPCE ( $\sim 12\%$ ) at around 560 nm. Furthermore, we found that the absorption spectrum of gold nanoparticles obtained after the consecutive photocurrent measurements for over 5000 s had no intrinsic changes compared to that before the measurements. Therefore, it is clear that the photocurrent was attributed not to the irreversible

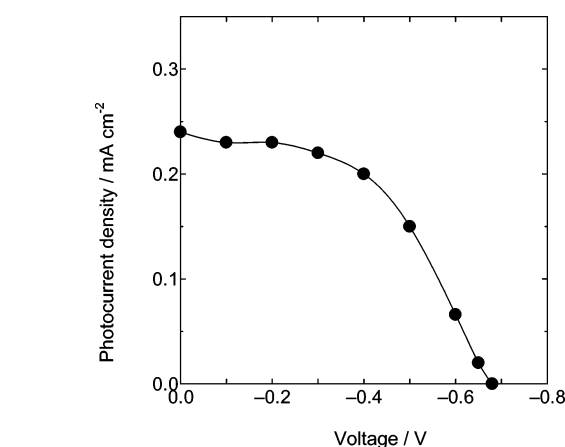


**Figure 5.** Photocurrent–voltage characteristics of the cell with the Au–TiO<sub>2</sub> film photoanode, a Au film cathode, and the acetonitrile–ethylene glycol solution containing 0.1 M LiNO<sub>3</sub>, 0.1 M FeCl<sub>2</sub>, and 0.05 M FeCl<sub>3</sub> under white light illumination ( $> 420$  nm, 10 mW cm<sup>-2</sup>).

oxidation (e.g., corrosion) of gold, but to the electron transport from the cathode via the Fe<sup>2+/3+</sup> redox couple. In addition, a TiO<sub>2</sub> film that has been treated with HAuCl<sub>4</sub> but not irradiated with UV light was also examined, and no photoresponses were obtained.

The photocurrent–voltage curve for the sandwich-type cell was examined under a Xe lamp (10 mW cm<sup>-2</sup>) (Figure 5). The fill factor (ff) was 0.50 and total energy conversion efficiency ( $\eta$ ) was 1.27%. Since these performances are currently much lower than those of the optimized dye-sensitized solar cell with an inorganic dye with organic ligands,<sup>24</sup> the present system should be optimized further for practical use.

Addition of 0.2 M 4-nitrobenzoic acid to the electrolyte further improved the maximum IPCE to 26%, probably because the adsorbed layer of 4-nitrobenzoic acid on TiO<sub>2</sub> blocks the surface levels and suppresses recombination.<sup>25</sup> Likewise, still there are possibilities to improve the performances. In the meantime, since the spectrum given in Figure 4 is a differential spectrum, from which the spectrum of TiO<sub>2</sub> has been subtracted, the absorbance does not reflect the overall photon absorption

(24) Nazeeruddin, M. K.; et al. *J. Am. Chem. Soc.* **2001**, *123*, 1613–1624.

(25) Yang, M.; Thompson, D. W.; Meyer, G. J. *Inorg. Chem.* **2000**, *39*, 3738–3739.



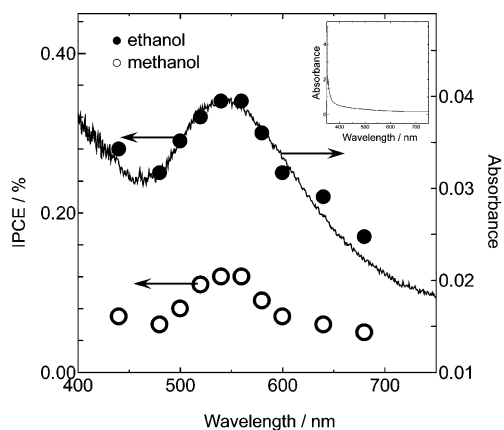


**Figure 6.** Action spectra for IPCE of the Au–TiO<sub>2</sub> film in the N<sub>2</sub>-saturated acetonitrile–ethylene glycol solution containing 0.1 M LiNO<sub>3</sub> and 0.5 M ethanol (or methanol) in response to visible light illumination ( $1.36 \times 10^{14}$  photons cm<sup>-2</sup> at each wavelength). Absorption spectrum of an unmodified TiO<sub>2</sub> film is given in the inset.

for all the gold nanoparticles in the film. The present TiO<sub>2</sub> film scatters light significantly (Figure 2A-a), and the gold nanoparticles inside absorb scattered photons also, although the absorption of the scattered light is not reflected by the absorbance in the differential spectrum. The absorption of the scattered light is well known to improve IPCE, so that opaque TiO<sub>2</sub> films are preferably used for dye-sensitized solar cells. From the spectrum of our Au–TiO<sub>2</sub> film (Figure 2A-b), 60% of the light could be absorbed by gold nanoparticles at the most. Therefore, the IPCE value of 26% is a possible value.

**Applicability to a Visible-Light-Sensitive Photocatalyst and a Photovoltaic Fuel Cell.** The photocatalytic ability of the Au–TiO<sub>2</sub> for oxidation of alcohols was examined. Figure 6 shows the photocurrent action spectra of the Au–TiO<sub>2</sub> film in the N<sub>2</sub>-saturated electrolyte with the addition of 0.5 M ethanol or 0.5 M methanol under visible light illumination. An anodic photocurrent was yielded at the Au–TiO<sub>2</sub> film as the visible light was irradiated, while the current was observed neither at a TiO<sub>2</sub> film under visible light irradiation nor at the Au–TiO<sub>2</sub> film when the light was turned off. Furthermore, the photocurrent action spectra closely fitted the absorption spectrum of the gold nanoparticles incorporated into the TiO<sub>2</sub> film, which shows the surface plasmon adsorption characteristic of gold nanoparticles. It indicates that both ethanol and methanol can be an electron donor for the Au–TiO<sub>2</sub> photoanode, although the IPCE values were about 0.30% and 0.12%, respectively. Incidentally, it is known that electrocatalytic activity for alcohol oxidation depends strongly on the electrode material.<sup>26</sup> The low efficiencies may be due to poor catalytic ability of gold for alcohol oxidation.<sup>27</sup> The efficiency could be improved by optimizing temperature, pH, and solvents or modification of the Au–TiO<sub>2</sub> film with an appropriate catalyst such as platinum.

The photoelectrochemical oxidation of alcohols was further studied. We first examined the photocatalytic oxidation of ethanol. The probable products of ethanol oxidation include acetaldehyde (CH<sub>3</sub>CHO), ethyl acetate (CH<sub>3</sub>COOCH<sub>2</sub>CH<sub>3</sub>), and acetic acid (CH<sub>3</sub>COOH). We measured short-circuit photocurrents in the presence of CH<sub>3</sub>CHO, CH<sub>3</sub>COOCH<sub>2</sub>CH<sub>3</sub>, and

CH<sub>3</sub>COOH at the Au–TiO<sub>2</sub> film in the N<sub>2</sub>-saturated electrolyte under white light irradiation (>420 nm, 10 mW cm<sup>-2</sup>). A photoanodic current was observed in the presence of either CH<sub>3</sub>CHO or CH<sub>3</sub>COOCH<sub>2</sub>CH<sub>3</sub>, while no obvious photocurrent was obtained in the presence of CH<sub>3</sub>COOH. Thus, we infer that the final product would be CH<sub>3</sub>COOH.

We also checked formaldehyde (HCHO), 2-methoxyethanol (CH<sub>3</sub>OCH<sub>2</sub>OH), formaldehyde dimethyl acetal (CH<sub>3</sub>OCH<sub>2</sub>OCH<sub>3</sub>), ethyle formate (HCOOCH<sub>3</sub>), and formic acid (HCOOH) as probable products of photocatalytic oxidation of methanol and concluded that the final product could be HCOOH.

In addition, O<sub>2</sub> was bubbled into the electrolyte containing 0.5 M ethanol. As a result, the anodic photocurrent gradually decreased and reached about 10% of the maximum photocurrent in 30 min. It is clear that O<sub>2</sub>, a typical electron acceptor, takes photoexcited electrons from the gold nanoparticles directly or via TiO<sub>2</sub> (described later) so as to interfere with the photoanodic current. Actually, H<sub>2</sub>O<sub>2</sub> was detected in the solution by using enzyme peroxidase and 2,2'-azinobis(3-ethylbenzothiazoline-6-sulfonic acid). This result supports the reduction of oxygen, since H<sub>2</sub>O<sub>2</sub> is one of the possible products of oxygen reduction.

These results indicate that the present Au–TiO<sub>2</sub> system is potentially applicable to a visible-light-sensitive photocatalyst that oxidizes ethanol and methanol at the expense of O<sub>2</sub> reduction. This is an exactly different phenomenon from that reported previously for photocatalysis at semiconductor–metal nanocomposites, in which metal nanoparticles have been used as a sink for charge carriers photoexcited in the semiconductor.<sup>16</sup> In addition, the present system is also potentially applicable to a photovoltaic fuel cell, in which photocurrents can be obtained with an alcohol and O<sub>2</sub>. Although IPCE of the recently reported enzyme-based photovoltaic fuel cell (about 35%)<sup>28</sup> is much higher than that of our system, potential advantages of our system might include stability (the lifetime is not limited by enzyme) and wide adaptabilities to temperature, pH, and solvents.

**Mechanisms of the Charge Separation.** The most important point in the mechanism of the present system is how the charges are separated. First, to examine the electron transfer from the gold nanoparticles to TiO<sub>2</sub>, we carried out spectroscopic measurements of the irradiated TiO<sub>2</sub>. It is known that TiO<sub>2</sub> is colored when a potential more negative than its flatband potential is applied.<sup>28</sup> Thus, if TiO<sub>2</sub> is colored under irradiation of the open-circuited Au–TiO<sub>2</sub> in the presence of an irreversible donor, it suggests that electrons are transferred from the irradiated gold to TiO<sub>2</sub> conduction band.

The absorbance changes at 680 nm were measured at a Au–TiO<sub>2</sub> film in a N<sub>2</sub>-saturated electrolyte solution containing 0.5 M ethanol as an irreversible donor under white light (>500 nm) irradiation (Figure 7). The absorbance at 680 nm of the Au–TiO<sub>2</sub> film gradually increased under white light and decreased quickly when O<sub>2</sub> was bubbled. In contrast, absorbance was completely constant when TiO<sub>2</sub> without Au was irradiated under the same conditions. The absorption band observed for Au–TiO<sub>2</sub> was quite broad over the visible range, indicating that the spectrum change was not due to the gold nanoparticles, but TiO<sub>2</sub>.<sup>29</sup> Actually, a similar spectrum change was observed when

(26) Zhou, W. J.; et al. *J. Power Sources* **2004**, *126*, 16–22.  
(27) Tremiliosi-Filho, G.; Gonzalez, E. R.; Motheo, A. J.; Belgsir, E. M.; Léger, J.-M.; Lamy, C. *J. Electroanal. Chem.* **1998**, *444*, 31–39.

(28) Garza, L.; Jeong, G.; Liddell, P.; Sotomura T.; Moore, T.; Moore, A.; Gust, D. *J. Phys. Chem. B* **2003**, *107*, 10252–10260.  
(29) Boschloo, G.; Fitzmaurice, D. *J. Phys. Chem. B* **1999**, *103*, 7860–7868.

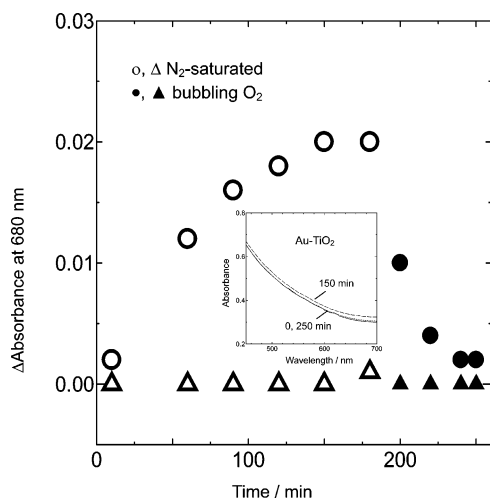


**Figure 7.** Changes in absorbance at 680 nm for the open-circuited Au–TiO<sub>2</sub> film (circles) and TiO<sub>2</sub> films (triangles) in a N<sub>2</sub>-saturated acetonitrile–ethylene glycol solution containing 0.1 M LiNO<sub>3</sub> and 0.5 M ethanol under 10 mW cm<sup>−2</sup> white light illumination (>500 nm) before (open circles and triangles) and after (filled circles and triangles) O<sub>2</sub> bubbling. Inset: Absorption spectra of the Au–TiO<sub>2</sub> film at 0, 150, and 250 min.

a potential negative of  $-0.9$  V was applied to the ITO electrode coated with the Ag–TiO<sub>2</sub>. Thus, it was verified that the photoexcited electrons at the gold particles are injected into the TiO<sub>2</sub> conduction band (Figure 1), and the injected electrons can be transferred to O<sub>2</sub> in turn. Since a Schottky barrier is formed at gold/TiO<sub>2</sub> junctions due to the large work function of gold<sup>30</sup> (Figure 1), observation of the electron transfer from the photoexcited gold to nonexcited TiO<sub>2</sub> is not surprising.

Next, the electron transfer from a donor to the gold particles was examined. Figure 8 shows the spectrum changes for the Au–TiO<sub>2</sub> film in the N<sub>2</sub>-saturated electrolyte without donor under 10 mW cm<sup>−2</sup> white light (>500 nm) irradiation. The visible light generated the photoexcited state of the gold nanoparticles due to the surface plasmon resonance, and the excited electrons were injected into the TiO<sub>2</sub> bulk. Hence, the gold nanoparticles lost electrons, resulting in a decrease of their absorbance, as shown by curve b in Figure 8. It is probable that the electrons and holes are spatially separated rapidly and electrostatically stabilized by counterions in the electrolyte. In the absence of an electron donor, the coloring of TiO<sub>2</sub> is negligible because the amount of injected electrons is so small. The injected electrons are gradually transferred back to the oxidized gold nanoparticles. However, with the addition of ethanol, an irreversible electron donor, the intact, photoresponsive gold nanoparticles are rapidly regenerated (curve c in Figure

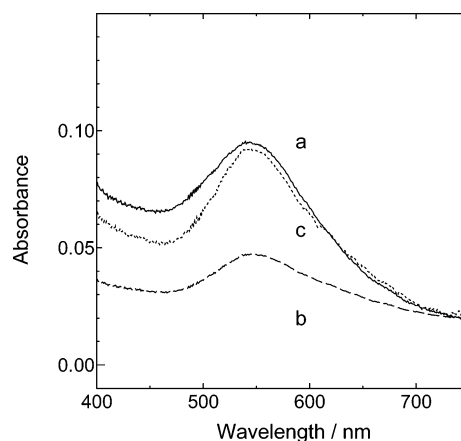


**Figure 8.** Absorption spectra of the Au–TiO<sub>2</sub> film in the N<sub>2</sub>-saturated electrolyte (the spectrum of TiO<sub>2</sub> has been subtracted). The open-circuited Au–TiO<sub>2</sub> film (a) was irradiated with white light (10 mW cm<sup>−2</sup>, >500 nm) for 30 min (b), and then ethanol (0.5 M) was added to the electrolyte (c).

8); electrons are transferred from the donor to the gold nanoparticles.

Accordingly, the mechanism of the plasmon-induced charge separation was clarified as follows: visible light generates the photoexcited state of the gold nanoparticles based on the surface plasmon resonance. Then the photoexcited electrons are injected into the TiO<sub>2</sub> bulk. Simultaneously, the oxidized gold nanoparticles take electrons from a donor in the solution (Figure 1).

## Conclusions

Charge separation at the plasmon-excited gold nanoparticles incorporated in TiO<sub>2</sub> was verified. It was found that the charge separation is accomplished by electron transfer from the excited gold particles to TiO<sub>2</sub> and that from a donor to the gold particle. As a low-cost photovoltaic cell, its incident photon to current conversion efficiency (IPCE) is 12% with the Fe<sup>2+/3+</sup> redox mediator. In addition, the Au–TiO<sub>2</sub> was newly found to function as a new class of visible-light-sensitive photocatalysts that oxidizes ethanol and methanol and reduces oxygen. Thus, a photovoltaic fuel cell is now one of its potential applications.

**Acknowledgment.** This work was supported in part by a Grant-in-Aid for Scientific Research on Priority Areas (417) from the Ministry of Education, Culture, Sports, Science and Technology of Japan. Y.T. thanks the Japan Society for the Promotion of Science (JSPS) for the postdoctoral fellowship.

**Supporting Information Available:** Complete refs 24 and 26. This material is available free of charge via the Internet at <http://pubs.acs.org>.

JA042192U

(30) Tang, J.; White, M.; Stucky, G. D.; McFarland, E. W. *Electrochem. Commun.* **2003**, 5, 497–501.